Study of entanglement in symmetric multi-quDits systems through information diagrams

Julio Guerrero[1,2⋆], Antonio Sojo[1], Alberto Mayorgas[3] and Manuel Calixto[2,3]

1 Department of Mathematics, University of Jaén,
Campus Las Lagunillas s/n, 23071 Jaén, Spain
2 Institute Carlos I of Theoretical and Computational Physics (iC1),
University of Granada, Fuentenueva s/n, 18071 Granada, Spain
3 Department of Applied Mathematics, University of Granada,
Fuentenueva s/n, 18071 Granada, Spain

⋆ jguerrer@ujaen.es

34th International Colloquium on Group Theoretical Methods in Physics
Strasbourg, 18-22 July 2022
doi:10.21468/SciPostPhysProc.14

Abstract

Along this paper, we analyze the entanglement properties of symmetric multi-quDits systems in a special type of states created from the generalization to $U(D)$ of the usual spin coherent states. By means of parity operators, we define what we call multicomponent Schrödinger cat states as parity adapted coherent states. Introducing the tool of information diagrams, i.e. representations of pairs of entropy measures, we analyze the correlation structure of this type of states and their M-wise reduced density matrices.

Copyright J. Guerrero *et al*.
This work is licensed under the Creative Commons
Attribution 4.0 International License.
Published by the SciPost Foundation.

Received 18-12-2022
Accepted 11-08-2023
Published 24-11-2023
Check for updates
doi:10.21468/SciPostPhysProc.14.029

1 Introduction

Information diagrams, simple representations based on a pair of entropic measures, are a helpful tool that can be used to analyze the correlation structure and mixture of a given quantum density matrix, and consequently the entanglement when applied to M-wise reduced density matrices.

On previous papers [1], we applied them to characterize the entanglement of parity adapted $U(D)$-spin coherent states (CSs) or DCATs. This work extends this analysis, computing information diagrams for the generalization to different parities of the purely even DCAT already studied.

To achieve this, we first review the concept of information diagrams in Section 2, then we define the generalization of DCAT using parity operators in Section 3, and eventually we combine both concepts to compute the information diagrams of the M-wise reduced density matrix (RDM) of these kind of states in Section 4.

2 Information diagrams and entropic measures

First, we will review the concept of information diagrams and its main properties. We will limit our scope since most details have already been given in [1] (and references therein).

Given a valid probability density function (PDF), we can compute the value of two different measures of information or entropy and plot a $2D$ point whose coordinates are those values. Information diagrams are the structure generated by this type of entropic representations when all valid PDF (or a subset thereof) are represented.

This idea can be generalized to quantum density matrices if we recall that their eigenvalues can be interpreted as probabilities, thus allowing the definition of a discrete PDF (for finite Hilbert spaces) that we can use to build up the information diagrams. In addition, if we select the two entropy measures as the normalized von Neumann $\mathcal{S}$ and linear entropies $\mathcal{L}$, we can directly compute them for a given density matrix ρ as:

$$\mathcal{S}(\rho) = -\operatorname{Tr}\rho \log_d \rho\,, \qquad \mathcal{L}(\rho) = \frac{d}{d-1}\left[1-\operatorname{Tr}\rho^2\right], \tag{1}$$

where d is the dimension of the Hilbert space associated with our quantum system.

As defined, these entropic measures are normalized, i.e., their value is 0 for pure states and 1 for maximally mixed states, and therefore we can ensure that the set of points $(\mathcal{L}(\rho),\mathcal{S}(\rho))$ generated by all valid density matrices ρ is a bounded set; however, it does not completely fill the entire unit square. The boundaries can be computed by means of variational methods as the search of curves with maximal or minimal von Neunman entropy given a fixed value of the linear entropy and a density matrix rank k. This allows the subdivion of the set into $d-2$ rank-dependent subregions. This makes possible the classification of density matrices within each subregion by the minimum rank they have. Details about the explicit meaning of these curves and their parametrization can be found on [1].

In Figure 1, we plotted the basic structure of an information diagram for quantum density matrices with $d = 5$. The global boundaries (in black) are the global extremal curves that enclose the entire set of allowed local points, within there are extremal curves (in grey) that give information about matrix ranks. The bottom-most curve represent all density matrices with rank $k = 2$, while each extremal curve moving upwards for increasingly higher ranks $k = 3,...,d$ set the minimum rank allowed on the whole area above it. Matrices with rank $k = 1$, i.e. pure states, are all located at the origin. It is also interesting to note that a density matrix located at the intersection point of the k-extremal curve with the global boundaries has k identical eigenvalues and $d-k$ zeros as it has maximal von Neumann entropy for its rank.

This rank based structure allows us to obtain an intuition about the level of entanglement and mixture of a family of density matrices. It is well-known [2] that density matrices which do not lie at the origin nor to the right of the NEMSs (Not Entangled Mixed States) Linear entropy[1] threshold (in dashed gray), all present entanglement. However, information diagrams do not give direct information about the absolute level of entanglement of a given density matrix.[2]

With all of this in mind, we will use information diagrams of RDMs to study the entanglement of what we call parity adapted coherent states of SU(D) or DCATS, a generalization of "Schrödinger cat states". In this case, information diagrams do provide useful information about entanglement and, in particular, the rank of the RDM is an entanglement monotone [3].

[1] A similar behaviour can be seen in the von Neumann Entropy.

[2] But if the system is divided in two parts and one of the parts is traced out, the location in the information diagram of the resulting RDM provides a good indicator of the level of entanglement of the original density matrix.

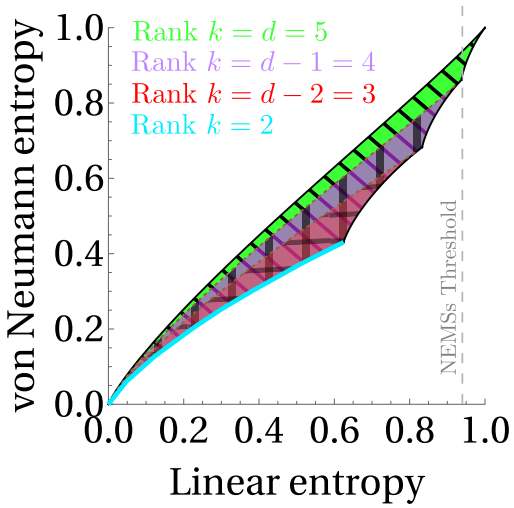

Figure 1: Information diagram for $d = 5$. Each region overlap with the ones below it.

3 Parity adapted U(D) CSs in symmetric multi-quDit systems

We shall introduce here the definition of parity adapted $U(D)$-spin coherent states (DCATS) in symmetric multi-quDit system. Before that, establishing the required mathematical tools is necessary.

We consider a system of N identical indistinguishable particles, each of which has D possible states or levels, e.g., N D-level identical atoms. Thus, we can define the creation (annihilation) operator for each level: $\{a_i^\dagger\}_{i=0}^{D-1}$ ($\{a_i\}_{i=0}^{D-1}$). Note that we denote the ground level as $i = 0$. As usual, these operators create (destroy) a particle on the i-th level $|i\rangle$.

In its fully symmetric representation, the collective $U(D)$-spin operators can be expressed as bilinear products of creation and annihilation operators, that is $S_{ij} = a_i^\dagger a_j$, $0 \leq i, j \leq D-1$ (Schwinger representation).

Note that the diagonal operators S_{ii} correspond to the number operator of the i-th level, while off-diagonal operators S_{ij} ($i \neq j$) are tunneling operators that move a particle from the j-th level $|j\rangle$ to the i-th level $|i\rangle$.

As this is the fully symmetric representation of $U(D)$, the associated space can be embedded into the Fock space $\mathcal{H}_F^{(N)}$ of dimension $d = \binom{N+D-1}{N}$, with a Bose-Einstein-Fock basis $\left\{|\vec{n}\rangle \in \mathcal{H}_F^{(N)} \,\middle|\, \|\vec{n}\|_1 = N\,, \langle\vec{n}|\vec{n'}\rangle = \delta_{\vec{n},\vec{n'}}\right\}$. Within this space, we pay special attention to the $U(D)$-spin coherent states (or DSCSs for short), which can be expressed as a multinomial form (see [1]) in terms of the $\{a_i^\dagger\}_{i=0}^{D-1}$ operators acting on the Fock vacuum.

However, for the sake of simplicity, we will use a more elementary (although equivalent) construction for DSCSs. Firstly, we define the one-particle state: $|\mathbf{z}\rangle^{(1)} = \frac{1}{\sqrt{1+|\mathbf{z}|^2}}\left[|0\rangle + \sum_{i=1}^{D-1} z_i\,|i\rangle\right]$, labeled with complex points $\mathbf{z} = (z_1, ..., z_{D-1}) \in \mathbb{C}^{D-1}$ without the coefficient $z_0 = 1$ (this election just represents the explicit choice of an specific local chart on the complex projective manifold defined by the normalized quantum states). The norm $|\mathbf{z}|$ is defined in terms of the scalar product $\mathbf{z}' \cdot \mathbf{z} = \sum_{i=1}^{D-1} \bar{z}_i' z_i$. The N particles $U(D)$-spin coherent states are simply defined as:

$$|\mathbf{z}\rangle^{(N)} = \bigotimes_{i=1}^{N} |\mathbf{z}\rangle_i^{(1)}\,, \tag{2}$$

where the superscript denotes number of particles, and the subscript represents the tag of each particle own space. It is obvious they are symmetric and that they do not present any entanglement as they are separable (tensor product states or TPS).

In addition, it is important to note that, in general, DSCSs are not orthogonal since their overlap is given by ${}^{(N)}\langle \mathbf{z}'|\mathbf{z}\rangle^{(N)} = \left[\frac{1+\mathbf{z}'\cdot\mathbf{z}}{\sqrt{(1+|\mathbf{z}'|^2)(1+|\mathbf{z}|^2)}}\right]^N$. This means that, even though they do not form a basis, they are an overcomplete continuous set of states that spans the entire space $\mathcal{H}_F^{(N)}$, i.e., they form a frame [4].

These non-entangled states can be combined to form highly entangled states by means of parity operators. These parity operators can be defined as $\Pi_j = \exp\{i\pi S_{jj}\}$, $j = 0, ..., D-1$ with $i^2 = -1$ being the imaginary unit. They measure the parity of the number of particles in the j-th level of a specific state. Note that $\Pi_i = \Pi_i^{-1}$. These operators generate the parity group of symmetric quDits systems $\mathbb{Z}_2 \times \overset{D}{...} \times \mathbb{Z}_2 = \mathbb{Z}_2^D$. However, as the number of particles N is fixed, $\Pi_0 \cdot ... \cdot \Pi_{D-1} = (-1)^N$ impose a constrain on the total parity $(-1)^N$, allowing us to discard one copy of $\mathbb{Z}_2$ and its corresponding parity operator. In particular, we select the one corresponding to the ground level (in correspondence with the choice $z_0 = 1$).

Parity operators act upon CSs such that they change the sign of the corresponding $\mathbf{z}$ components,

$$\Pi_i |\mathbf{z}\rangle^{(N)} = \Pi_i |z_1, ..., z_i, ..., z_{D-1}\rangle^{(N)} = |z_1, ..., -z_i, ..., z_{D-1}\rangle^{(N)} . \tag{3}$$

We define the following parity operators: $\Pi_j^{b_j} = \exp\{i\pi b_j S_{jj}\}$ and $\Pi^{\mathbb{b}} = \Pi_1^{b_1}\Pi_2^{b_2} \cdot ... \cdot \Pi_{D-1}^{b_{D-1}}$, where $\mathbb{b} = (b_1, b_2, ..., b_{D-1}) \in \{0,1\}^{D-1}$ is a binary string of length $D-1$ that labels elements of the parity group $\mathbb{Z}_2^{D-1}$. They allow us to define the definite parity subspace projectors as the Fourier transform in the $\mathbb{Z}_2^{D-2}$ group,

$$\Pi_{\mathbb{c}} = 2^{1-D} \sum_{\mathbb{b}\in\{0,1\}^{D-1}} (-1)^{\mathbb{b}\cdot\mathbb{c}} \Pi^{\mathbb{b}}, \tag{4}$$

where $\mathbb{c} = [c_1, c_2, ..., c_{D-1}] \in \{0,1\}^{D-1}$ is the parity of the subspace that this projector projects to. They can be used to project states to a defined parity $\mathbb{c}$ subspace, thus allowing us to define the $\mathbb{c}$-parity adapted CSs states or $\mathbb{c}$-parity DCAT as:

$$|\mathrm{DCAT}_{\mathbb{c}}(\mathbf{z})\rangle^{(N)} = \frac{1}{\mathcal{N}_{\mathbb{c}}^{(N)}(z)} \Pi_{\mathbb{c}} |\mathbf{z}\rangle^{(N)} = \frac{2^{1-D}}{\mathcal{N}_{\mathbb{c}}(\mathbf{z})} \sum_{\mathbb{b}\in\{0,1\}^{D-1}} (-1)^{\mathbb{b}\cdot\mathbb{c}} \left|\mathbf{z}^{\mathbb{b}}\right\rangle^{(N)}, \tag{5}$$

where $\mathbf{z}^{\mathbb{b}} := ((-1)^{b_1} z_1, ..., (-1)^{b_i} z_i, ..., (-1)^{b_{D-1}} z_{D-1})$ and

$$\left[\mathcal{N}_{\mathbb{c}}^{(N)}(\mathbf{z})\right]^2 = 2^{1-D} \sum_{\mathbb{b}\in\{0,1\}^{D-1}} (-1)^{\mathbb{b}\cdot\mathbb{c}} \frac{[1+\mathbf{z}^{\mathbb{b}}\cdot\mathbf{z}]^N}{(1+|\mathbf{z}|^2)^N}, \tag{6}$$

is a normalization factor or the norm of the unnormalized DCAT.

As an example, we provide the explicit expression of the $\mathbb{c}$-parity DCAT state and $\mathcal{N}_{\mathbb{c}}(\mathbf{z})$ for $D = 2, 3$ (qubits and qutrits).

For $D = 2$, there are only two possible levels, and one component of $\mathbf{z}$ and parities; thus $\mathbf{z} = \alpha$ and $\mathbb{c} = c$. Any one-particle coherent state $|\mathbf{z}\rangle^{(1)} := |\alpha\rangle^{(1)}$ is written as $|\alpha\rangle^{(1)} = \frac{|0\rangle+\alpha|1\rangle}{\sqrt{1+|\alpha|^2}}$, and the corresponding N-particle $\mathrm{2CAT}_c$ is expressed as

$$|\mathrm{2CAT}_c(\alpha)\rangle^{(N)} = \frac{1}{2\mathcal{N}_c^{(N)}(\alpha)} \left[|\alpha\rangle^{(N)} + (-1)^c |-\alpha\rangle^{(N)}\right], \tag{7}$$

with:

$$\left[\mathcal{N}_c^{(N)}(\alpha)\right]^2 = \frac{1}{2}\frac{(1+|\alpha|^2)^N + (-1)^c(1-|\alpha|^2)^N}{(1+|\alpha|^2)^N} = \frac{1}{2}\left[1 + (-1)^c \left(\frac{1-|\alpha|^2}{1+|\alpha|^2}\right)^N\right]. \tag{8}$$

It is easy to check that $\Pi^b \left|2\text{CAT}_c(\alpha)\right\rangle^{(N)} = (-1)^{c\cdot b} \left|2\text{CAT}_c(\alpha)\right\rangle^{(N)}$ as it corresponds to its parity. It is also important to note that, for $c = 1$, the $2\text{CAT}_1(0)$ can only be defined as the limit $\alpha \to 0$ of the normalized DCAT, since the normalization factor tends to zero as the unnormalized state itself also does.

For $D = 3$, there are three possible levels and two component of $\mathbf{z}$ and parities; thus $\mathbf{z} = (\alpha, \beta)$ and $\mathbb{c} = [c_1, c_2]$. A one-particle coherent state $|\mathbf{z}\rangle^{(1)} := |\alpha, \beta\rangle^{(1)}$ is written as $|\alpha, \beta\rangle^{(1)} = \frac{|0\rangle + \alpha|1\rangle + \beta|1\rangle}{\sqrt{1+|\alpha|^2+|\beta|^2}}$, with the corresponding N-particle $3\text{CAT}_{\mathbb{c}}$ expressed as:

$$\begin{aligned} \left|3\text{CAT}_{\mathbb{c}}(\alpha,\beta)\right\rangle^{(N)} = \frac{1}{4\mathcal{N}_{\mathbb{c}}^{(N)}(\alpha,\beta)}\Big[&\left|\alpha,\beta\right\rangle^{(N)} + (-1)^{c_1}\left|-\alpha,\beta\right\rangle^{(N)} \\ &+ (-1)^{c_2}\left|\alpha,-\beta\right\rangle^{(N)} + (-1)^{c_1+c_2}\left|-\alpha,-\beta\right\rangle^{(N)}\Big], \end{aligned} \tag{9}$$

with:

$$\begin{aligned} \left[\mathcal{N}_{\mathbb{c}}^{(N)}(\alpha,\beta)\right]^2 = \frac{1}{4} &+ \frac{(-1)^{c_1}(1-|\alpha|^2+|\beta|^2)^N + (-1)^{c_2}(1+|\alpha|^2-|\beta|^2)^N}{4(1+|\alpha|^2+|\beta|^2)^N} \\ &+ \frac{(-1)^{c_1+c_2}(1-|\alpha|^2-|\beta|^2)^N}{4(1+|\alpha|^2+|\beta|^2)^N}. \end{aligned} \tag{10}$$

It is easy to check that $\Pi^{\mathbb{b}} \left|3\text{CAT}_{\mathbb{c}}(\alpha,\beta)\right\rangle^{(N)} = (-1)^{\mathbb{c}\cdot\mathbb{b}} \left|3\text{CAT}_{\mathbb{c}}(\alpha,\beta)\right\rangle^{(N)}$ as it corresponds to the partial parity of the given pair.

These expressions will be used in Section 4 to compute the eingenvalues of the corresponding M-wise RDM $\rho_{\mathbb{c}}^{(M)}(\mathbf{z}) = \text{Tr}_{(N-M)}\left[\left|\text{DCAT}_{\mathbb{c}}(\mathbf{z})\right\rangle\left\langle\text{DCAT}_{\mathbb{c}}(\mathbf{z})\right|\right]$, which allows us to analyze the entanglement structure of the DCATs using information diagrams.

4 Entropic measures of reduced density matrices

As we have seen in Section (2), we can compute von Neumann and linear entropies associated to any quantum state using the eingenvalues of the corresponding density matrix operator.

This allow us to compute the entropies associated to the M-wise RDM of a DCAT state (i.e. partial tracing $N-M$ out of the N particles). Using the explicit expression of DCATs in terms of the Fock basis [1], one can easily compute the RDM taking partial trace. This RDM can be diagonalized and then its entropy computed [6].

For the sake of simplicity, we will limit ourselves, again, to $D = 2, 3$. As it is not relevant here, we omit the diagonalization and directly provide the eingenvalues of the RDM. We consider the partial trace of $N - M > N/2$ particles, leaving $M \leq N/2$ on our state (cases where $M > N/2$ are symmetric to the case $M \leq N/2$ by interchanging $M \to N - M$). This means that the M-wise RDM is associated with the Fock space $\mathcal{H}_F^{(M)} \neq \mathcal{H}_F^{(N)}$ with dimension $d_M = \binom{M+D-1}{M} < d_N = \binom{N+D-1}{N}$.

For $D = 2$, we provide the eingenvalues of the RDM as a vector, and we omit the expression of eigenvectors, which are not relevant here,

$$\rho_c^{(M)}(\alpha) = \left(\frac{\left[L_+^{N-M} + (-1)^c L_-^{N-M}\right]\left[L_+^M + L_-^M\right]}{2L_+^N\left[\mathcal{N}_c^{(N)}\right]^2}, \frac{\left[L_+^{N-M} - (-1)^c L_-^{N-M}\right]\left[L_+^M - L_-^M\right]}{2L_+^N\left[\mathcal{N}_c^{(N)}\right]^2}, \vec{0} \right), \tag{11}$$

where $L_\pm := 1 \pm |\alpha|^2$ and $\vec{0}$ is a vector that pads the diagonal with zeros until the required dimension is reached. In general, we only have two non-zero eingenvalues.

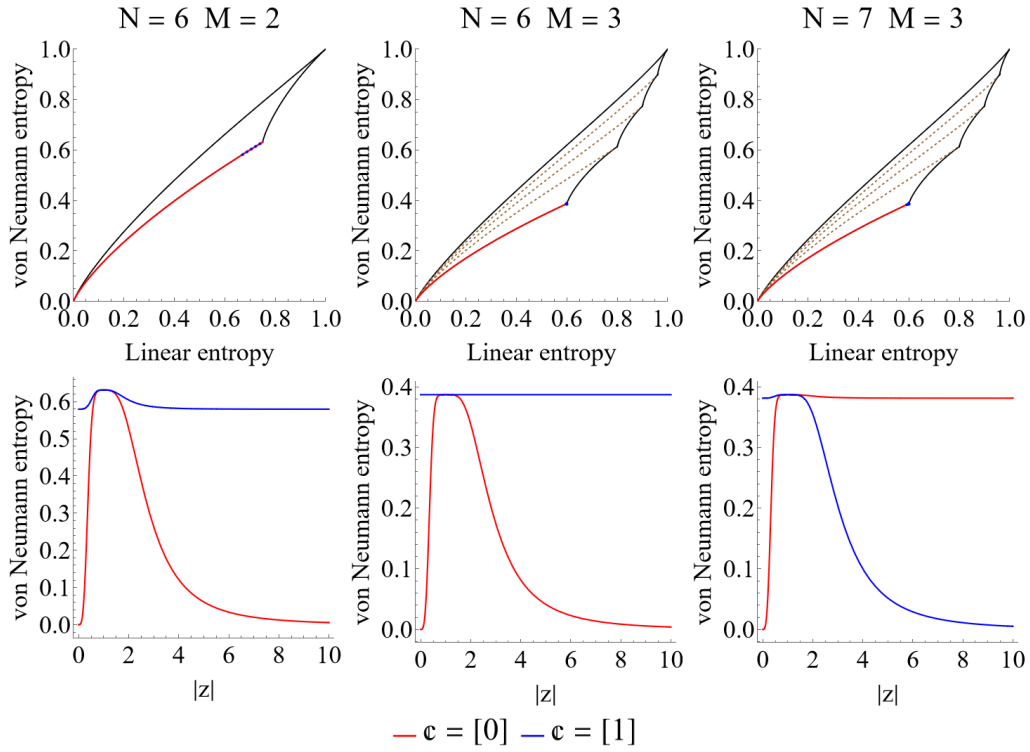

Figure 2: Information diagrams (upper line) for $D = 2$, $N = 6, 7$ and $M = 2, 3$, and the corresponding plots (bottom line) of the von Neumann entropy as a function of the parameter $|z|$.

In Figure (2), we plotted the von Neumann entropy as a function of the absolute value of the complex parameter z as well as the associated information diagrams for three pairs of (N, M) and both possible parities $\mathbb{c} = [0], [1]$.

At $z = 0$, the $\mathbb{c} = [0]$ RDM presents no entropy, while $\mathbb{c} = [1]$ starts from a high value of the entropy. As $|z|$ increases, so does the entropy for both cases and any pair (N, M) of particles until the peak value is reached at $|z| = 1$. At this point, it can be shown that any derivative of order $< M$ vanishes. This means that the higher M is, the flatter the peak will be. From this point, the entropy decreases for both parities with one of them consistently over the other. For even N, $\mathbb{c} = [1]$ remains at the top while this behaviour reverses if N is odd.

Using the previous information, we can give an interpretation to each corresponding information diagram. For $D = 2$, the maximum value of the rank is $k = 2$ for all $M > 1$ since all RDM lie on the bottom-most curve. However, $k = 1$ is reached for RDM with no entropy and, therefore, no entanglement (pure states). For even N, only $\mathbb{c} = [0]$ covers the entire possible entropy range (entropy is normalized to dimension $d_M = M$ for $D = 2$), while $\mathbb{c} = 1$ only spans a narrow interval of possible values. On the other hand, for odd N,the entire range is available for both parities.

For $D = 3$, we have:

$$\rho_{\mathbb{c}}^{(M)}(\alpha,\beta) = \frac{1}{4L_{++}^{N}\left[\mathcal{N}_{\mathbb{c}}(\alpha,\beta)\right]^2} \tag{12}$$
$$\times\Big(\Big[L_{++}^{N-M}+(-1)^{c_1}L_{-+}^{N-M}+(-1)^{c_2}L_{+-}^{N-M}+(-1)^{c_1+c_2}L_{--}^{N-M}\Big]\Big[L_{++}^{M}+L_{-+}^{M}+L_{+-}^{M}+L_{--}^{M}\Big],$$
$$\Big[L_{++}^{N-M}-(-1)^{c_1}L_{-+}^{N-M}+(-1)^{c_2}L_{+-}^{N-M}-(-1)^{c_1+c_2}L_{--}^{N-M}\Big]\Big[L_{++}^{M}-L_{-+}^{M}+L_{+-}^{M}-L_{--}^{M}\Big],$$
$$\Big[L_{++}^{N-M}+(-1)^{c_1}L_{-+}^{N-M}-(-1)^{c_2}L_{+-}^{N-M}-(-1)^{c_1+c_2}L_{--}^{N-M}\Big]\Big[L_{++}^{M}+L_{-+}^{M}-L_{+-}^{M}-L_{--}^{M}\Big],$$
$$\Big[L_{++}^{N-M}-(-1)^{c_1}L_{-+}^{N-M}-(-1)^{c_2}L_{+-}^{N-M}+(-1)^{c_1+c_2}L_{--}^{N-M}\Big]\Big[L_{++}^{M}-L_{-+}^{M}-L_{+-}^{M}+L_{--}^{M}\Big],\vec{0}\Big),$$

where $L_{\sigma_1\sigma_2} := 1+\sigma_1|\alpha|^2+\sigma_2|\beta|^2$ with $\sigma_i \in \{-1,+1\}$.

Now, in Figure 3, we show a contour plot of the von Neumann entropy as a function of the point $(|\alpha|,|\beta|)$, as well as the corresponding information diagram for fixed $N = 7$ and $M = 2$ and all relevant parities (the $\mathbb{c} = [1,0]$ case is symmetric to $\mathbb{c} = [0,1]$ with the interchange $\alpha \leftrightarrow \beta$). The color scale represent the von Neumann entropy in both contour plots and information diagrams.

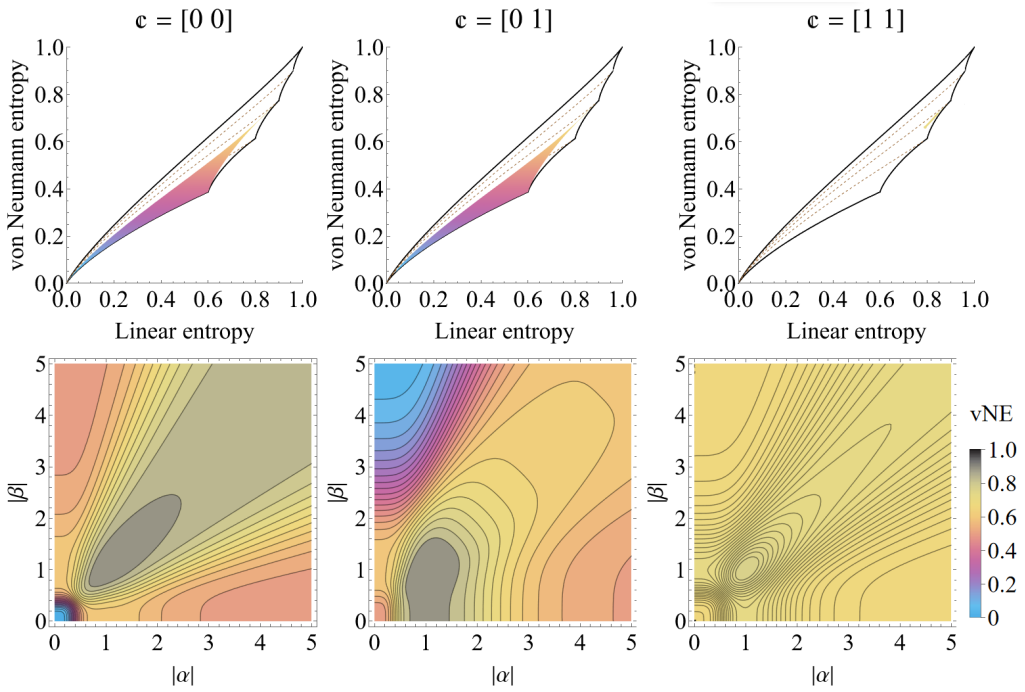

Figure 3: Information diagrams (upper row) for $D = 3$, $N = 7$, $M = 2$, and all relevant parities, and the corresponding contour plots (bottom row) representation of the von Neumann entropy as a function of the parameters $(|\alpha|,|\beta|)$.

For $D = 3$, the behaviour is similar to $D = 2$ but the number of possible cases increases exponentially. For even N, the higher the number of 1's a parity has, the higher the associated average entropy is (higher on the information diagram), and the narrower the range is occupied. For odd N and all parities except $\mathbb{c} = [1,1]$, the entire possible entropy range is occupied taking into account the maximum rank available. Each one of the two axis $(|\alpha|,|\beta|)$ has an intimate relation with its corresponding parity component. If the parity components are not equal, an asymmetry between both axis is created as not all directions are equivalent, decreasing the entropy at points near the axises with corresponding non-zero parity component.

Again, all the properties can be directly visualized on the information diagrams in Figure 3. Now, the possible ranks scale from $k = 1$ to $k = 4$ for any M, and completely even parities occupy higher areas (with non null measure) on the diagrams.

5 Conclusion

Parity adapted coherent states or DCATs can be physically produced on Kerr materials [5] or as products of Bose-Einstein condensates and have applications on models such as the Lipkin-Meshkov-Glick model [1]. Therefore the entanglement structure of this kind of states is of high interest.

This work is limited in scope but in [6] the ideas seen here are further developed, generalizing the decomposition of the RDM of DCATs into their eigenvectors using Group theoretical methods and more sophisticated interpretations.

6 Acknowledgements

Funding information We thank the support of the Spanish MICINN through the projects PGC2018-097831-B-I00 and PID2022-138144NB-I00, and Junta de Andalucía through the projects UHU-1262561, FQM-381 and FEDER/UJA-1381026. AM thanks the Spanish MIU for the FPU19/06376 predoctoral fellowship. AS thanks University of Jaén for a contract under the project FEDER/UJA-1381026.

References

[1] J. Guerrero, A. Mayorgas and M. Calixto, *Information diagrams in the study of entanglement in symmetric multi-quDit systems and applications to quantum phase transitions in Lipkin-Meshkov-Glick D-level atom models*, Quantum Inf. Process. **21**, 223 (2022), doi:10.1007/s11128-022-03524-7.

[2] K. Życzkowski, P. Horodecki, A. Sanpera and M. Lewenstein, *Volume of the set of separable states*, Phys. Rev. A **58**, 883 (1998), doi:10.1103/physreva.58.883.

[3] R. Horodecki, P. Horodecki, M. Horodecki and K. Horodecki, *Quantum entanglement*, Rev. Mod. Phys. **81**, 865 (2009), doi:10.1103/RevModPhys.81.865.

[4] A. Vourdas, *Analytic representations in quantum mechanics*, J. Phys. A: Math. Gen. **39**, R65 (2006), doi:10.1088/0305-4470/39/7/R01.

[5] S. Arjika, M. Calixto and J. Guerrero, *Quantum statistical properties of multiphoton hypergeometric coherent states and the discrete circle representation*, J. Math. Phys. **60**, 103506 (2019), doi:10.1063/1.5099683.

[6] J. Guerrero, A. Sojo, A. Mayorgas and M. Calixto, *Schmidt decomposition of parity adapted coherent states for symmetric multi-quDits*, J. Phys. A: Math. Theor. **56**, 355304 (2023), doi:10.1088/1751-8121/aceae0.